7. For a reaction condition of 5% $Pd(OAc)_2$/2.5 *i*-Pr_2NEt/1.2 *n*-Bu_4NCl/ DMF, see Larock, R. C.; Baker, B. E. *Tetrahedron Lett.* **1988**, *29*, 905. For a reaction condition of Pd $(PPh_3)_4/Et_3N/CH_3CN$ see, Negishi, E.; Zhang, Y.; O'Conner, B. *Tetrahedron Lett.* **1988**, *29*, 2915. For a reaction condition of $Pd(OAc)_2/PPh_3/Ag_2CO_3$ see, Ableman, M. R.; Oh, T.; Overman, L. E. *J. Org. Chem.* **1987**, *52*, 4133.

Investigation of Desolvation Process in Argon Inductively Coupled Plasma

Yong-Nam Pak*, Young-Min Cho, Gae-Ho Lee†, and Hyo-Jin Kim‡

**Department of Chemistry, Korea National University of Education, Cheong-won, Chung-buk 363-791, Korea*
†Department of Chemistry, College of Natural Sciences, Chungnam University, Taejon 305-764, Korea
‡Department of Pharmacy, Dong Duck Women's University, Seoul 136-714,Korea

Received June 17, 1996

Atomic spectrometry has long provided excellent qualitative and quantitative trace element analysis. Recent developments, involving "non-flame" techniques such as furnace Atomic Absorption (AA), Inductively Coupled Plasma (ICP)-Atomic Emission Spectrometry (ICP-AES) as well as Mass Spectrometry (ICP-MS), have improved detection to the sub-ppb level. Despite the success of flame and plasma atomic spectrometry, elemental analysis is still limited in understanding the fundamental processes in an atomic source.[1]

Typically, a droplet is generated in a nebulizer and enters into an atomic source. And it goes through evaporation, melting, vaporization, excitation as well as ionization following molecular reactions such as molecular formation and dissociation. Various types of reactions and interferences can be involved in each step that has a very pronounced effect upon measuring the observed signal intensity, which is converted to the number of atoms or ions and finally to concentration. Any side reactions or interferences could happen during the processes and give erroneous results. Characterization and optimization is only possible when each step is studied separately. The nature of the source can be understood better and experimental parameters intelligently optimized only when each step is well characterized. To alleviate the interferences and more importantly to improve the analytical ability of atomic source, it is essential to understand the processes occuring in an atomic source.

Though there are a lot of experimental researches, relatively little investigations have been performed in the mechanistic study of the atomization processes. At the most, in atomic spectroscopy, studies have been limited to flames. Clampitt[2] showed that desolvation in an air-acetylene is due to the heat transfer process. Thermal conductivity plays the key role in desolvation of several aqueous and organic solvents. Bastiaans[3] has extended the desolvation of solvent model to vaporization of solute particles in an air-acetylene flame successfully. Hieftje[4] has proposed two models, heat and mass transfer, for the calculation of particle vaporization rate in a flame. Chen and Pfender[5~7] investigated that the Knudsen effect plays a significant role in heat transfer process for a particle vaporization in a thermal plasma. However, the studies have been focused on the vaporization process and the desolvation process in ICP has not been studied yet.

In this report, desolvation process is investigated for Ar Inductively Coupled Plasma. Earlier theoretical models used in the flame and plasma to describe a vaporization process have been successfully applied to describe the desolvation process in ICP. Calculated desolvation rate constant (k_d) has been compared with experimental one to determine which model describes the desolvation process the best. The desolvation rate of solvent has been determined by observing the first appearance of sodium emission (Na bullet). The distance between two bullets (those of the dried and wet aerosol) has been converted to the time taken for desolvation. Comparison of experimental and calculated results show that a simple heat transfer or mass transfer desolvation alone can not explain the desolvation process in ICP.

With a simple experiment, valuable information on the desolvation process in ICP could be obtained. For the matter of simplicity, modeling is restricted to water. This report is a preliminary study and a detailed investigation is further needed to understand the process completely.

Theory

Intuitively, one can consider that the rate of evaporation of the solute might be governed either by the rate at which energy (heat) can be transported to the solute surface or, alternatively, by the rate at which solute material can leave that surface. These cases are termed heat-transfer or mass transfer-limiting, respectively.

Heat-Transferred Evaporation. When thermal equilibrium is assumed between a droplet and the surrounding gases, *i.e.* when the temperature of the surface of a volatilizing droplet is constant during the evaporation process and the droplet is immersed in an infinite, stagnant medium, the rate of heat conducted through the medium to the surface is

$$dQ/dt = 4\pi r^2 h_c (T_g - T_s) \tag{1}$$

where h_c is the heat-transfer coefficient, r is the radius of the droplet, T_g is the plasma gas temperature, and T_s is the temperature of the droplet surface. The heat transfer coefficient is defined as

$$hc = \frac{\lambda N_s}{2r}\left[\frac{\ln(1+\Delta H_{av}/\Delta H_v)}{\Delta H_{av}/\Delta H_v}\right] = \frac{\lambda N_s}{2r}\Lambda \tag{2}$$

where Λ is the mass counter-flow coefficient, Ns is the Nusselt number, and λ is the thermal conductivity of the vapor or plasma gas, whichever is lower. The bracketed term is included to account for resistance to heat flow to the droplet

surface because of mass counter flow. *Ns* is related to heat convection to the particle surface. When the droplet velocity is nearly the same as that of the plasma gas, the Nusselt number approaches its minimum value of 2.[8]

The rate of heat loss can be expressed as

$$\frac{dQ}{dt}=\frac{\Delta H_v}{M}\left(\frac{-dm}{dt}\right)+4\pi r^2\varepsilon_s\sigma T_s^4 \tag{3}$$

where the first term represents the energy consumed by the species during evaporation from the particle surface and the second term defines the amount of energy lost by radiation from the droplet. In the present study, the second term has little effect and the calculated value is less than 3% of the first term. Combining equation 1 and 3, one can integrate from time 0 to t while radius changes from r_0 to r and the rate expression becomes

$$r^2=r_0^2-\left[\frac{2M\Lambda\lambda(T_g-T_s)}{\Delta H_v\rho}\right]t \tag{4}$$

where r_0 is the initial droplet radius and the bracketed term can be expressed as k_d, the heat transfer desolation rate constant. The evaporation of combustible fuel droplets follows a similar expression as shown by other investigators.[9,10]

Knudsen Effect corrected Heat-Transfer Evaporation. The Knudsen effect predicts that the rate of heat transfer to the droplet will be reduced as the droplet dimension become small with respect to the mean free path of the vapor. The Knudsen number is defined as $Kn=L/2r$ where L is the mean free path of the gas species and r is the droplet radius. For $Kn<0.001$, the Knudsen effect is negligible and is called "continuum region". For $Kn>10$, free molecular flow region, mass transfer based on the kinetic theory only applies. At intermediate region where $1<Kn<10$, "temperature jump regime", heat-transfer is partly substituted by mass transfer evaporation. Chen and Pfender[6] have shown how heat-transfer is modified by the Knudsen effect. The true rate of heat transfer Q_k calculated from the early Q in the continuum regime is given as;

$$Q_k=\frac{Q}{(1+Z/r)} \tag{5}$$

Where Z is a parameter called temperature jump distance;

$$Z=\left(\frac{2-\alpha}{a}\right)\left(\frac{r}{1+r}\right)\left(\frac{2}{\mathrm{Pr}}\right)L \tag{6}$$

where a is the thermal accommodation coefficient, γ is the specific heat ratio, and Pr is the Prandtl number. The thermal accommodation coefficient, α, defines the effectiveness with which kinetic energy from gas species impinging on the droplet surface is transferred to the particle. For small droplets, the Knudsen effect becomes progressively more important and reduces the rate of heat transfer. In the limit, the effective heat transfer becomes zero and only mass transfer process controls evaporation.

Mass-Transferred Evaporation. Monchick and Reiss[11] developed an equation that governs evaporation:

$$-\frac{dm}{dt}=\frac{4\pi r^2M\alpha P_s}{(2\pi MRT_g)^{1/2}(1-\alpha/2)\left[1+\frac{\alpha vr}{(1-\alpha/2)D}\right]} \tag{7}$$

where α is the "evaporation coefficient", P_s is the vapor pressure of the solvent at the droplet surface, R is the gas constant, D is the diffusion coefficient, and v is the velocity of molecules leaving (or striking) droplet surface. It is straight forward to integrate and the result is

$$r=r_o-\left[\frac{M\alpha P_s}{\rho(2\pi MRT_g)^{1/2}(1-\alpha/2)}\right]t \tag{8}$$

when r becomes very small that αvr could be ignored. The rate of molecular release at the droplet surface becomes limiting.

Experiment

A 100 ppm NaCl solution is nebulized into ICP and the initial appearance of sodium emission, typically called as a sodium bullet, is observed. Then a completely dried sample aerosol is sent to ICP and the difference in the height of the sodium bullet is recorded. The difference in the height corresponds to the length (and time) of desolvation process taken by the sample aerosol. To obtain a completely dried sample, a heater combined with a condenser (−20 ℃) followed by an argon cryogenic trap is employed. To measure the difference between dried and wet aerosol, image of the plasma was focused unto a screen by a convex lenz of which focal length is 40 mm. Then the change of height could be measured simply using a ruler. The distance measured is 2.4 mm. It is not important if the top or the bottom of the bullet is observed. The distance can be also measured by observing sodium emission line using a spectrometer. Since the current commercial spectrometer moves a mirror to choose the observation height, resolution is deteriorated and limited to 1 mm.

Results and Discussion

Desolvation rate constant k_d can be calculated using equation 4 for the heat transfer controlled desolvation process. All the parameters used in calculation is listed in Table 1. One of the parameters that affects on k_d most significantly is thermal conductivity. Since a droplet is surrounded by the plasma gas, conductivity of argon, λ_{Ar}, will control the heat flux. However, as droplet is evaporated and surrounded by vapor, thermal conductivity can be changed to that of vapor, λ_{vap}. Table 2 shows that the desolvation rate constant is more controlled by the lesser one-thermal conductivity of vapor. Since the smaller conductivity governs the incoming of heat flux, desolvation rate calculated using the thermal conductivity of water vapor agrees better with the experimental one.

When a large droplet of which diameter is large compared to the mean free path of molecules leaving its surface, the rate of desolvation can be controlled by the rate at which thermal energy can reach the droplet surface. Under this condition, the thermal conductivity and heat capacity of the thin, stagnant film surrounding the droplet become important. However, when the droplet's surface becomes of the order of the mean free path of molecules, that behavior changes. As the process is developed, the vapor is warmed up and heat can reach the droplet at a more than sufficient

Table 1. Physical Parameters Used for Calculation of Desolvation Rate Constant for Water

Parameter			Ref
λ	Thermal Conductivity	127.16 g.cal/cm.s.K	12
Ns	Nusselt Number	2	8
ΔH_{ov}	Overall Heat of Conversion Cp(Tg-Ts)	81.153 Kcal/mol.K	13
ΔH_v	Heat of Vaporization	9770 cal/mole	14
Ts	Surface Temperature	100 ℃	
Tg	Gas Temperature	6,000 K	assumed
a	Thermal Accomodation Coefficient	0.8	6
γ	Specific Heat Ratio	1.667	assumed
L	Mean Free path	1.5 μm	calculated
α	Evaporation Coefficient	0.015	15
Ps	Saturation Vapor Pressure	1.013×10^6 dyne/cm^2	assumed
R	Ideal Gas Constant	8.3144 J/mol.K	

Table 2. Comparison of Experimental Evaporation Rate Constant with Calculated Constants of Heat and Mass Transfer Evaporation Model

	Heat-transfer (mm^2/s)	Knudsen Effect corrected Heat-Transfer (mm^2/s)	Mass Transfer (mm/s)
k_d(Calculated)			
λ_{Ar}	0.296	0.0629	
λ_{vap}	0.0870	0.0185	
			0.0367*
k_d(Experimental)	0.0207(mm^2/s)		0.863(mm/s)

*α=0.015 is used. If α is 0.35, calculated mass transfer desolvation constant become 0.863.

rate, there is no temperature gradient until one reaches a distance from the surface approximating the mean free path. This region where the gradient exists as the "thermal jump distance". Under these conditions, droplet evaporation can be viewed as being limited by the rate at which the surrounding gas molecules transfer energy to the droplet through "thin" region. Heat conduction to the droplet surface is limited by this thin film as the diameter of droplet decreases; Knudsen effect prevails. Equation 5 and 6 are used for the calculation of desolvation rate with Knudsen effect correction. In this preliminary report, Q_k is calculated at the onset of a desolvation of a droplet with 2.5 μm diameter.

The data provided in Table 2 strongly predicts the evidence of Knudsen effect corrected heat transfer desolvation. In the previous study of droplet desolvation in the flame, Clampitt[2] showed that the heat transfer process alone predict well for the behavior of evaporation. However, the size of droplets are very large (around 30-40 μm) compared to the ones studied in this research. When a droplet is large, most of desolvation process is governed by the heat transfer process and a simple heat transfer model can describe the desolvation behavior well. As a droplet is getting smaller, the heat transfer evaporation is not valid any more because of the reduced incoming heat flux.

As the droplet diminishes during the desolvation, the radius becomes so small that it will fall into the free molecular-flow region (Kn>10). This region is not well described and there is no proper theory to explain the phenomena in this region. It is only assumed in this study that the free molecular region is so small that it does not affect on the total desolvation time.

Another process of desolvation that should be considered is mass transfer, which becomes important when a droplet becomes very small because the mass flux per unit area would be very large and the rate of molecule release at the surface become limiting for a small droplet. Current theories on the mass transfer include a parameter "evaporation coefficient(α)" which indicates the ease of release of molecule from the droplet surface. When the empirical value 0.015 determined by Hirth[15] is used for the calculation, k_d is 0.0367 mm/s which is more than 20 times slower compared with the experimental value. What it suggests to us is that the desolvation is less likely controlled by the mass transfer process alone. It doesn't necessarily mean that the mass transfer does not occur at all but it could be that only the degree of mass transfer is not so large. Large evaporation coefficient (α=0.35) can be used so as to predict the experimental value. However, the theoretical ground for determining α is not valid.

One can combine heat transfer and mass transfer model together to explain the total desolvation process. In the earlier study of vaporization of alkali particles in a flame, Hieftje[4] suggested the combined model where large particle volatilization is controlled by the rate of heat conduction and the small particle vaporization is rate limited by the mass transfer. However, it was not successful to predict where the break in behavior occur. Whether it is a Knudsen effect corrected heat transfer or a combined heat and mass transfer process, desolvation is not solely due to the heat transfer but it is partly changed to mass transfer character as the radius becomes close to the mean free path. Actually, two models are quite close with each other. The concept used in "thermal jump distance" can be viewed as part of mass transfer process. The former view provides more of continuos transitions while the latter gives an abrupt change but conceptually clearer explanations.

To determine if a model dominates desolvation process entirely, the whole life of droplet should be examined. Only when the radius of droplet is plotted with the life time, then it will be more precisely concluded if there is only one or two processes exist (or dominate) as well as if transition occurs. If two processes exist and transit during the desolvation, radius with time (or r^2 with time) would not be a linear function. In order to perform the research, it is imperative to introduce mono-dispersed aerosols. This work is underway in our laboratory.

In conclusion, desolvation rate of water droplets in Ar ICP could be measured with a simple Na bullet test and the results are compared with existing models of evaporation. Heat transfer controlled process alone could not predict the behavior. Knudsen effect corrected heat transfer controlled gave the best agreement with the experimental results, which means that the rate of heat conduction decreased as

the size decreases even in the case of desolvation. To be able to predict more precisely when and how much Knudsen effect contributes to desolvation, the entire life of mono-dispersed droplets should be monitored and this study is underway in our laboratory.

Acknowledgment. The authors are grateful for the financial support by the Korean Science and Engineering Foundation (94-0800-03-02).

References

1. Boorn, A. W.; Cresser, M. S.; Browner, R. F. *Spectrochim. Acta*, **1980**, *35B*, 823.
2. Clampitt, N. C.; Hieftje, G. M. *Anal. Chem.* **1972**, *44*, 1211.
3. Bastiaans, G. J.; Hieftje, G. M. *Anal. Chem.* **1974**, *46*, 901.
4. Hieftje, G. M.; Wittig, E.; Pak, Y.; Miller, J. M. *Anal. Chem.* **1987**, *59*, 2867.
5. Chen, X.; Pfender, E. *Plasma Chem. Plasma Process.* **1982**, *2*, 293.
6. Chen, X.; Pfender, E. *Plasma Chem. Plasma Process.* **1983**, *3*, 97.
7. Chen, X.; Pfender, E. *Plasma Chem. Plasma Process.* **1982**, *3*, 351.
8. Russo, R. E.; Hieftje, G. M. *Anal. Chim. Acta*, **1980**, *118*, 293.
9. Hottel, H. C.; Williams, G. C.; Simpson, H. C. *Fifth Symposium on Combustion*; Reinhold: New York, 1955; 101.
10. Bahn, G. S. *Advances in Chemistry Series*, **1958**, *2*, 104.
11. Monchick, L.; Reiss, H. *J. Chem. Phys.* **1954**, *22*, 831.
12. Hirshfelder, J. O.; Curtiss, C. O.; Bird, R. B. *Molecular Theory of Gases and Liquids*; Wiley & Sons: New York, N. Y., 1954; p 526.
13. *JANAF*, 2nd ed.; U. S. Government Printing Office: Washington, D. C., 1971.
14. *International Critical Tables*, 1st ed.; McGraw-Hill: New York and London, 1926.
15. Hirth, J. P. *In the Characterization of High Temperature Vapors*; Margrave, J. L., Ed.; Wiley: New York, 1967; p 453.

Determination of Electron Transfer Kinetics at Ferrocenecarboxamidoyl Monolayer/Solution Interface

Hun-Gi Hong

Department of Chemistry, Sejong University, Seoul 133-747, Korea

Received June 17, 1996

Monomolecular film of self-assemblies[1~7] has been used as a model system to understand complex interfacial phenomena such as wetting, adhesion, friction, catalysis and electron/energy transfer on biological membrane. The electron transfer kinetics at the redox-polymer/ solution interface have been already extensively studied in both theoretical and experimental approaches by Saveant, Anson, Murray, Albery and their coworkers.[8~12] However, there are only a few reports[1a,13,14] on the electron transfer in self-assembled electroactive monolayers. Recently, we reported electrochemical measurements of electron transfer rates on the redox-active molecule-terminated film based on zirconium phosphonate.[15] This note reports indirect determination of kinetic parameters for the mediated electron transfer reaction between ferrocenecarboxamidoyl monolayer film and solution species. In order to get the kinetic information on monolayer-coated electrode system, it is essential to take into account simultaneously a few factors which can limit current. The rate constant for electron-cross exchange (k_{ex}), standard rate constant ($k°$) and symmetry factor (α) which were related to several limiting factors such as mass transfer, electron-exchange and charge transport were determined from observed limiting currents (i_{obs}) by digital simulation using three parameters-fit least squares.

Results and Discussion

The sequential adsorption procedure[6,15] was used to prepare gold rotating disk electrode modified with electroactive ferrocenecarboxamidoyl monolayer. This modified Au electrode typically gives well-defined surface waves (shown in Figure 1) in which peak current is linearly proportional to scan rate (data not shown) and peak potential separation was smaller than 30 mV independent of scan rate between 20 and 200 mV/s. The surface formal potential ($E^{o'}_s$) of ferro-

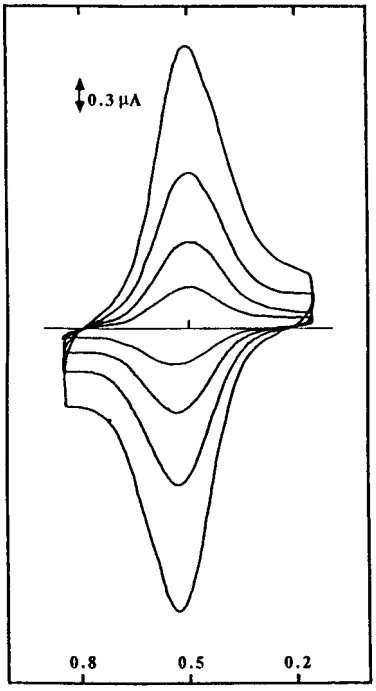

Figure 1. Cyclic voltammograms of ferrocene-modified Au electrode in 0.1 M $NaClO_4$. Potential, V *vs.* SCE.